Available online at www.sciencedirect.com
SCIENCE DIRECT®
Journal of Solid State Chemistry 178 (2005) 1620–1629
JOURNAL OF SOLID STATE CHEMISTRY
www.elsevier.com/locate/jssc

# Crystal structure, hydrogen absorption properties and crystal structure of the deuterides of some Nb–Ni derived $\mu$ phase compounds

J.-M. Joubert*

*Laboratoire Chimie Métallurgique des Terres Rares, CNRS, 2-8 rue Henri Dunant, F-94320 Thiais Cedex, France*

Received 1 February 2005; received in revised form 21 February 2005; accepted 28 February 2005

**Abstract**

Ternary compounds in the Nb–Ni–V system with the structure of the $\mu$ phase (structure type $W_6Fe_7$, $R\bar{3}m$) have been investigated as regards their hydrogenation properties as a function of V content. On the other hand, the crystal structures of the $\mu$ phase deuterides $Nb_{57}Ni_{43}D_{44}$ ($Nb_{7.2}Ni_{5.8}D_{5.03}$, $R\bar{3}m$, $a = 5.103(1)$ Å, $c = 27.649(3)$ Å, $Z = 3$, $R_{Bragg} = 11.6\%$), $Nb_{42}Ni_{31}V_{27}D_{64}$ ($Nb_{5.32}Ni_{4.08}V_{3.6}D_{8.73}$, $R\bar{3}m$, $a = 5.136(1)$ Å, $c = 27.815(3)$ Å, $Z = 3$, $R_{Bragg} = 7.5\%$) and $Nb_{48}Ni_{23}Al_{29}D_{36}$ ($Nb_{6.27}Ni_{2.93}Al_{3.8}D_{4.37}$, $R\bar{3}m$, $a = 5.113(1)$ Å, $c = 27.926(3)$ Å, $Z = 3$, $R_{Bragg} = 7.4\%$) have been studied by powder neutron diffraction and are discussed in terms of the metal atom distribution in the metallic substructure, the latter being established by means of joint refinement of neutron and X-ray diffraction data.


*Keywords:* Metal hydrides; Crystal structure; Intermetallic compounds; Neutron diffraction; Joint Rietveld refinement; Site occupancy; Frank–Kasper phases

## 1. Introduction

The $\mu$ phase is an intermetallic compound pertaining to the group of Frank–Kasper (also called topologically close packed) phases. Its crystal structure is rhombohedral (space group $R\bar{3}m$) typified by $W_6Fe_7$. The ideal atomic distribution is as follows (in hexagonal setting): W in sites $6c_1$ (0, 0, $z = 0.167$), $6c_2$ (0, 0, $z = 0.346$), $6c_3$ (0, 0, $z = 0.448$), and Fe in sites $3a$ (0, 0, 0) and $18h$ ($x = 0.833$, $\bar{x}$, $z = 0.167$) [1]. The $\mu$ phase has in several systems an extended homogeneity domain. After a powder diffraction study in several binary systems, it has been shown that the non-stoichiometry is accommodated by substitutional disorder on several sites depending on the composition [2,3]. The first evidence of hydrogen absorption in a $\mu$ phase was reported in Ref. [4] for the compound $Nb_{51.5}Ni_{48.5}$ which absorbs 0.1 H/M (hydrogen atom per metal atom). In order to improve the hydrogenation capacity, the effects of stoichiometry changes and ternary substitutions are studied in a systematic way. The hydrogenation properties have been examined in the binary Nb–Ni system as a function of the composition across the homogeneity domain ($Nb_{49.6}Ni_{50.4}$–$Nb_{56.9}Ni_{43.1}$) and in the ternary Nb–Ni–Al system as a function of Al content (up to $Nb_{46.6}Ni_{22.1}Al_{31.3}$), showing a substantial increase of the hydrogen uptake up to 0.5 H/M [5]. Vanadium, like aluminum, has a large solubility in the Nb–Ni $\mu$ phase. In the present work, an investigation of the hydrogenation properties of the Nb–Ni–V $\mu$ phase is conducted as a function of V composition (samples $Nb_{49}Ni_{43}V_8$, $Nb_{46}Ni_{37}V_{17}$, $Nb_{43}Ni_{30}V_{27}$ and $Nb_{41}Ni_{26}V_{33}$). The distribution of the three metal atoms among the five sites is obtained by joint refinement of neutron and X-ray diffraction data for compounds in the two ternary Nb–Ni–V and Nb–Ni–Al systems at the maximum V or Al content ($Nb_{42}Ni_{31}V_{27}$ and $Nb_{48}Ni_{23}Al_{29}$).

*Corresponding author. Fax: +33 1 49 78 12 03.
*E-mail address:* jean-marc.joubert@glvt-cnrs.fr.

0022-4596/$ - see front matter © 2005 Elsevier Inc. All rights reserved.
doi:10.1016/j.jssc.2005.02.027

Finally, the crystal structures of the deuterides of these two compounds are studied by neutron diffraction together with the structure of the deuteride of the binary $Nb_{57}Ni_{43}$ compound. Though having a limited importance from the point of view of hydrogen storage, the presence of only tetrahedral interstices characteristic of a Frank–Kasper phase allows to discriminate between geometric and chemical affinity effects during hydrogenation process.

## 2. Experimental

The intermetallic compounds have been synthesized by arc melting of the pure elements in an argon atmosphere. Annealing treatments were carried out in silica tubes sealed under secondary vacuum, the alloys being protected from the contact with silica by means of a tantalum foil. Annealing conditions were 1050 °C and 14 days ($Nb_{57}Ni_{43}$ and $Nb_{42}Ni_{31}V_{27}$) or 7 days (other Nb–Ni–V alloys). The Nb–Ni–Al sample was annealed in a high frequency induction furnace under dynamic secondary vacuum at 1140 °C during 8 h. The intermetallic compounds were characterized by metallographic examination and electron probe micro-analysis (EPMA, Cameca SX100). Powder X-ray diffraction diagrams were obtained at room temperature on a D8 Advance (Bruker AXS) diffractometer working in the $\theta-\theta$ Bragg–Brentano geometry (spinning sample 30 rpm, $2\theta$ range 8–120°, step-scan intervals 0.04° ($2\theta$) chosen according to the sample line widths, time per step 20–60 s, Cu$K\alpha$, backscattered rear graphite monochromator, scintillation detector). The measurement of the hydrogenation properties was performed on a conventional Sievert's apparatus equipped with a 100 bar pressure gauge (accuracy 0.5% full scale). The estimated accuracy for capacity measurement is 0.03 H/M. The same device was used for the deuterium loading of the samples prior to neutron diffraction. This was done at room temperature in an especially designed stainless steel container (tube, outer diameter 9.5 mm, inner diameter 7.8 mm) able to withstand and keep high deuterium pressures up to 100 bar. The samples were charged close to this pressure and the capacity (hereafter called nominal capacity) was measured. Powder neutron diffraction experiments were performed at the Laboratoire Léon Brillouin (common laboratory CEA-CNRS) in Saclay, France on the 3T2 instrument at room temperature (Debye–Scherrer geometry, $2\theta$ range 6–126°, step-scan intervals 0.05° ($2\theta$), 24 h scan, $\lambda = 1.224$ Å, $^3$He multi-detector (20 cells)). The Nb–Ni sample was measured after deuteration under 100 bar while Nb–Ni–V and Nb–Ni–Al samples were measured in the stainless-steel container before and after the introduction of deuterium. The non-deuterated samples were analyzed by joint Rietveld refinement of X-ray and neutron powder diffraction patterns in order to obtain the atomic distribution of the three atoms on the different sites. This was performed by constraining the total composition to match the analyzed composition and the full occupancy of each site according to the method described in Ref. [2] adapted in the case of ternary compounds. Eight occupancy parameters were therefore primarily refined. This number may be reduced when slightly negative values for the parameters are found. In such a case, occupancy values are fixed to zero. Considering the large uncertainties associated with the refinement of the displacement parameters due to the micro-absorption effect in the case of X-ray diffraction data, those parameters are not given for the intermetallic compounds.

Since it is very unlikely to be modified during the hydrogenation, the distribution of the metal atoms was conserved in the refinement of the deuterated samples focusing on the location and occupancy of the deuterium insertion sites. All the possible insertion sites were derived geometrically after the study of the coordination polyhedron of each metal atom. As a consequence for a Frank–Kasper phase, they are all tetrahedral. The position and radius ($r$) of the insertion site was defined as the center and radius of the largest sphere in contact with the four coordination metal atoms. A home-made program was used to calculate these values, taking into account the radius of the metal atoms. In case of metal sites shared by different atoms, the radii weighted by the occupancy parameters were used. All the possible sites were successively tried and discarded from the refinement if the occupancy factor is refined negatively. The atomic coordinates of deuterium were refined only in the case of a sufficiently high occupancy of the given site.

All the structure refinements were achieved by the Rietveld method using the program Fullprof [6] with the following conditions: background interpolated between peaks, pseudo-Voigt profile function, coherent neutron scattering values $b_{Nb} = 7.05$ fm, $b_{Ni} = 10.30$ fm, $b_V = 0.38$ fm, $b_{Al} = 3.45$ fm, $b_D = 6.67$ fm. The secondary phases were taken into account with a structural model when giving peaks in the diffraction patterns and the weight amount was refined. The stainless-steel (austenitic, $Fm\bar{3}m$, $a = 3.953$ Å) container used for the neutron diffraction measurements was treated in the pattern-matching mode (no intensity constraint) due to the impossibility to handle properly the texture of the tube.

## 3. Results

Fig. 1 shows the phase diagram of the Nb–Ni–V ternary system at 1050 °C as published by Eremenko et al. [7]. The large extension of the $\mu$ phase in the

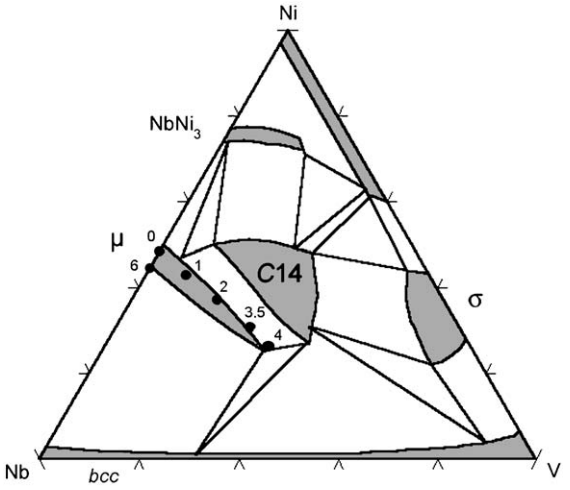


Fig. 1. Isothermal section of the Nb–Ni–V phase diagram at 1050 °C [7]. The synthesized compositions in the $\mu$ phase homogeneity domain have been represented as dots and numbered according to Table 1. The composition of the binary sample $Nb_{51.5}Ni_{48.5}$ (0) [2] is indicated as well as a reference.

Nb–Ni binary system and in the ternary field is roughly represented. Four samples (1–4) have been synthesized with increasing amounts of vanadium. One may note that the homogeneity domain is neither parallel to the Nb–V nor to the Ni–V axis indicating that single phase alloys can not be achieved by a simple substitution of one of the two elements of the binary Nb–Ni $\mu$ phase by vanadium. For this reason, though following a straight line in the ternary composition diagram, the synthesized compositions do not keep constant any of the element concentrations.

The chemical and structural characterization of all the samples can be found in Table 1. The three samples with vanadium content between 8 at% (1) and 27 at% (3) are found to be single phase. Both *a* and *c* lattice parameters show an increase as a function of vanadium content (not shown). The cell volume is drawn in Fig. 2. The result for the binary sample $Nb_{51.5}Ni_{48.5}$ (0) from Ref. [2] is given for comparison. $Nb_{41}Ni_{26}V_{33}$ (4) composition with 20 wt% of C14 secondary phase does definitely not lie in the homogeneity domain of the $\mu$ phase. According to these results, a new sample was synthesized for the purpose of doing neutron diffraction experiment. Its composition was chosen to be $Nb_{42}Ni_{31}V_{27}$ (5), close to $Nb_{43}Ni_{30}V_{27}$ (3) but slightly poorer in Nb in order to avoid the precipitation of the bcc phase. In this latter sample, traces of the C14 phase are observed showing the narrow width of the $\mu$ phase domain in this region of the phase diagram.

The atomic distribution of the three atom kinds on the five different sites cannot be obtained from a single diffraction set. However, owing to the relatively small X-ray diffraction contrast between V and Ni, Nb distribution can be refined and is indicated in Table 1 and Fig. 3. The Nb composition has been constrained to the analyzed composition by EPMA. A pseudo-atom averaging the Ni and V electronic densities has been used in the refinement. The complete distribution has been obtained for the binary $Nb_{57}Ni_{43}$ (6) by X-ray diffraction and for the ternary $Nb_{42}Ni_{31}V_{27}$ (5) studied by joint analysis of X-ray and neutron powder diffraction data, again with a constraint to the analyzed composition. A relative agreement is obtained concerning the Nb distribution for the two samples with similar compositions $Nb_{43}Ni_{30}V_{27}$ (3) and $Nb_{42}Ni_{31}V_{27}$ (5). The atomic distribution has also been obtained for a sample in the Nb–Ni–Al system ($Nb_{48}Ni_{23}Al_{29}$) by the same technique. All the results are gathered in Table 1 and shown graphically on Figs. 4 and 5.

The pressure–composition hydrogen absorption curves of the Nb–Ni–V samples have been measured at room temperature. They are shown in Fig. 6. One may note the large increase of the hydrogen capacity as a function of vanadium content.

Deuterium loading does not differ much from hydrogen loading. The capacities under 100 bar ($Nb_{57}Ni_{43}D_{44}$, $Nb_{42}Ni_{31}V_{27}D_{64}$, $Nb_{48}Ni_{23}Al_{29}D_{36}$ to be compared with $Nb_{56.9}Ni_{43.1}H_{52}$ [5], $Nb_{43}Ni_{30}V_{27}H_{60}$ (this work) and $Nb_{46.6}Ni_{22.1}Al_{28.8}H_{41}$ [5]) and the pressure–composition curves (not shown) do not change significantly. The crystal structures of the three deuterides $Nb_{57}Ni_{43}D_{44}$, $Nb_{42}Ni_{31}V_{27}D_{64}$ and $Nb_{48}Ni_{23}Al_{29}D_{36}$ have been refined from powder neutron diffraction. All the samples are single phase except $Nb_{48}Ni_{23}Al_{29}D_{36}$ in which traces of $Nb(Al)D_2$ are found resulting from the hydrogenation of the bcc supplementary phase in the sample. This phase was taken into account in the refinement with a structure model according to Ref. [8]. A preliminary analysis yields the conclusion that the $\mu$ phase structure is not deeply modified apart from a significant cell parameter increase. All the atomic positions of the (all tetrahedral) insertion sites were calculated and are reported in Table 2 together with the site radii. The deuterium occupancies for all the sites were progressively refined. The atomic positions for the metal atoms were refined but are not observed to change significantly. The results are presented in Table 3. An example of refinement is given in Fig. 7. In each case, the refined deuterium content is in good agreement with the nominal composition of the deuterides. The refinements are satisfactory for each sample in spite of the strong contribution from the sample holder. Relatively worse reliability factor ($R_{Bragg}$) is observed in the case of $Nb_{57}Ni_{43}D_{44}$ in spite of several attempts to improve the refinement (including a refinement of the metal distribution otherwise fixed to the values found in the non-hydrogenated sample). Displacement parameters for metal atoms are comparatively high and could perhaps

Table 1
Characterization of the intermetallic compounds. Indicated are: nominal composition, sample number, analyzed composition by EPMA, nature and phase amount (wt%) of secondary phases, lattice parameters of the $\mu$ phase ($R\bar{3}m$), atomic positions, atomic distribution on the sites in atom per site ($^*$ distribution of Ni and V not determined) and reliability factor of the Rietveld refinement

| Nominal composition (at%) | $Nb_{49}Ni_{43}V_8$ | $Nb_{46}Ni_{37}V_{17}$ | $Nb_{43}Ni_{30}V_{27}$ | $Nb_{41}Ni_{26}V_{33}$ | $Nb_{42}Ni_{31}V_{27}$ | $Nb_{48}Ni_{23}Al_{29}$ | $Nb_{57}Ni_{43}$ |
|---|---|---|---|---|---|---|---|
| Sample number | 1 | 2 | 3 | 4 | 5 | | 6 |
| Analyzed composition (at%) | $Nb_{47.4(3)}Ni_{44.1(4)}V_{8.4(4)}$ | $Nb_{44.8(3)}Ni_{37.6(2)}V_{17.6(2)}$ | $Nb_{41.1(3)}Ni_{30.8(2)}V_{28.1(2)}$ | $Nb_{39.1(5)}Ni_{29.7(8)}V_{31.3(7)}$ | $Nb_{40.9(5)}Ni_{31.4(6)}V_{27.7(4)}$ | $Nb_{48.2(2)}Ni_{22.5(8)}Al_{29.3(8)}$ | $Nb_{55.3(3)}Ni_{44.7(3)}$ |
| Secondary phases | | Traces of unreacted Nb | bcc $Nb_{\sim 85}V_{\sim 15}$ (1 wt%) $a = 3.260$ Å<br>Traces of unreacted Nb | bcc $Nb_{\sim 60}V_{\sim 40}$ (traces)<br>$C14$ $Nb_{33.1(3)}Ni_{29.4(3)}V_{37.5(2)}$ (~20 wt%)<br>Traces of unreacted Nb | $C14$ $Nb_{33}Ni_{31}V_{35}$ (traces) | bcc (6 wt%) | bcc $Nb_{96}Ni_4$ (2 wt%) |
| $a$ (Å) | 4.920(1) | 4.934(1) | 4.949(1) | 4.947(1) | 4.941(1) | 5.008(1) | 4.954(1) |
| $c$ (Å) | 26.765(5) | 26.833(3) | 26.905(3) | 26.912(8) | 26.859(2) | 27.233(2) | 26.978(3) |
| $V$ (Å$^3$) | 561.1(1) | 565.6(1) | 570.7(1) | 570.3(1) | 567.9(1) | 591.5(1) | 573.4(1) |
| $3a$ (0, 0, 0)<br>CN 12 | Nb 0.68(6)$^*$ | Nb 0.06(5) $^*$ | Nb 0 $^*$ | Nb 0 $^*$ | Nb 0<br>Ni 0.65(2)<br>V 2.35(2) | Nb 0<br>Ni 1.06(4)<br>Al 1.94(4) | Nb 2.16(7)<br>Ni 0.84(7) |
| $6c_1$ (0, 0, $z$)<br>CN 15 | $z = 0.1660(3)$<br>Nb 6 $^*$ | $z = 0.1660(3)$<br>Nb 6$^*$ | $z = 0.1653(3)$<br>Nb 6 $^*$ | $z = 0.1632(5)$<br>Nb 5.8(1) $^*$ | $z = 0.1652(2)$<br>Nb 5.38(5)<br>Ni 0.28(5)<br>V 0.34(5) | $z = 0.1662(2)$<br>Nb 5.87(4)<br>Ni 0<br>Al 0.13(4) | $z = 0.1654(3)$<br>Nb 5.91(7)<br>Ni 0.09(7) |
| $6c_2$ (0, 0, $z$)<br>CN 16 | $z = 0.3468(3)$<br>Nb 5.85(9) $^*$ | $z = 0.3486(3)$<br>Nb 6$^*$ | $z = 0.3503(3)$<br>Nb 5.62(6) $^*$ | $z = 0.3494(6)$<br>Nb 5.4(1) $^*$ | $z = 0.3504(2)$<br>Nb 5.84(4)<br>Ni 0<br>V 0.16(4) | $z = 0.3507(3)$<br>Nb 5.93(4)<br>Ni 0<br>Al 0.07(4) | $z = 0.3472(3)$<br>Nb 5.86(7)<br>Ni 0.14(7) |
| $6c_3$ (0, 0, $z$)<br>CN 14 | $z = 0.4520(4)$<br>Nb 5.32(8) $^*$ | $z = 0.4526(3)$<br>Nb 5.84 (7) $^*$ | $z = 0.4533(3)$<br>Nb 4.41(6) $^*$ | $z = 0.4545(6)$<br>Nb 4.0(1) $^*$ | $z = 0.4525(3)$<br>Nb 4.73(4)<br>Ni 0<br>V 1.27(4) | $z = 0.4547(2)$<br>Nb 5.88(4)<br>Ni 0<br>Al 0.12(4) | $z = 0.4521(3)$<br>Nb 5.25(7)<br>Ni 0.75(7) |
| $18h$ ($x$, $\bar{x}$, $z$)<br>CN 12 | $x = 0.836(2)$<br>$z = 0.2569(4)$<br>Nb 0.64(9) $^*$ | $x = 0.834(2)$<br>$z = 0.2580(1)$<br>Nb 0 $^*$ | $x = 0.837(2)$<br>$z = 0.2584(1)$<br>Nb 0 $^*$ | $x = 0.840(3)$<br>$z = 0.2603(6)$<br>Nb 0 $^*$ | $x = 0.834(1)$<br>$z = 0.2575(2)$<br>Nb 0<br>Ni 11.32(5)<br>V 6.68(5) | $x = 0.833(1)$<br>$z = 0.2574(3)$<br>Nb 1.12(4)<br>Ni 7.74(4)<br>Al 9.14(4) | $x = 0.834(1)$<br>$z = 0.2562(3)$<br>Nb 2.42(7)<br>Ni 15.58(7) |
| $\chi^2$ | 2.5 | 2.3 | 2.2 | 3.6 | 5.5 | 10.2 | 4.3 |
| $R_{Bragg}$ (%) X-ray<br>neutron | 5.9 | 4.6 | 5.6 | 9.3 | 5.0<br>5.7 | 8.0<br>6.5 | 5.9 |

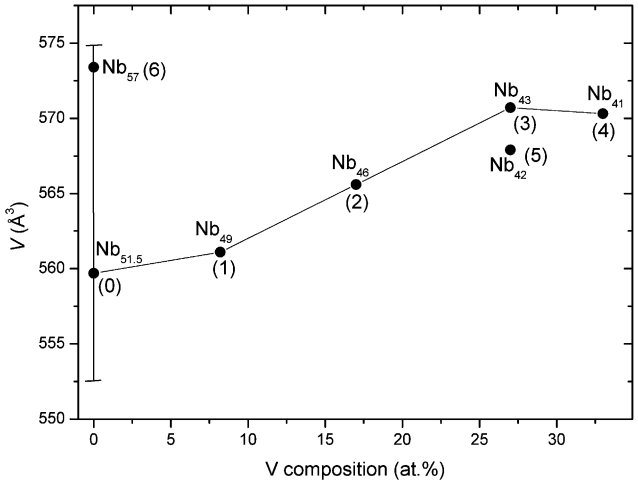


Fig. 2. Cell volume of the $\mu$ phase as a function of the nominal vanadium composition. The niobium content and sample number is indicated for each sample (the value for $Nb_{51.5}Ni_{48.5}$ (0) and the variation of the cell volume in the binary homogeneity domain indicated as a vertical line is from Ref. [2]). The error bars are smaller than the dot size.

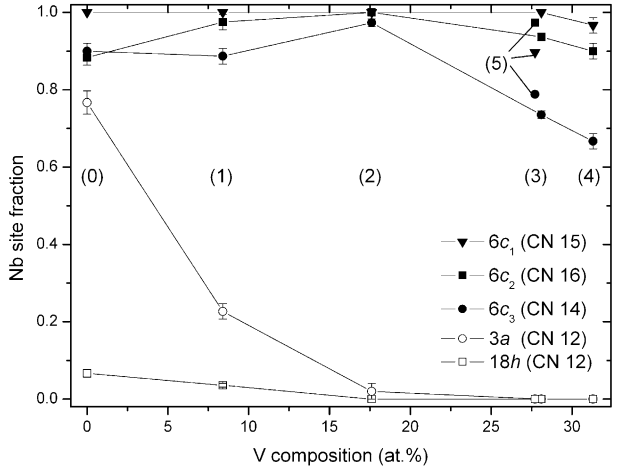


Fig. 3. Nb site fraction from X-ray powder diffraction refinement on the five sites of the $\mu$ phase in the Nb–Ni–V system as a function of composition. Data points for the binary compound $Nb_{51.5}Ni_{48.5}$ [2] and for the ternary compound $Nb_{42}Ni_{31}V_{27}$ (5) obtained by joint X-ray and neutron diffraction refinement (non-linked symbols) have been added for comparison.

be explained by a lower symmetry due to non-symmetric moves of the metal atoms. The ratio between the number of parameters to be refined in a subgroup and the number of independently measured reflections is too high. Thus, we preferred to refine the structure in the given model, which is, at least, a valid average structure.

The cell volumes of the three compounds as a function of the hydrogen content are presented in Fig. 8. The same slopes are observed indicating a good consistency between the nominal deuterium content and lattice parameters for the three samples. One may

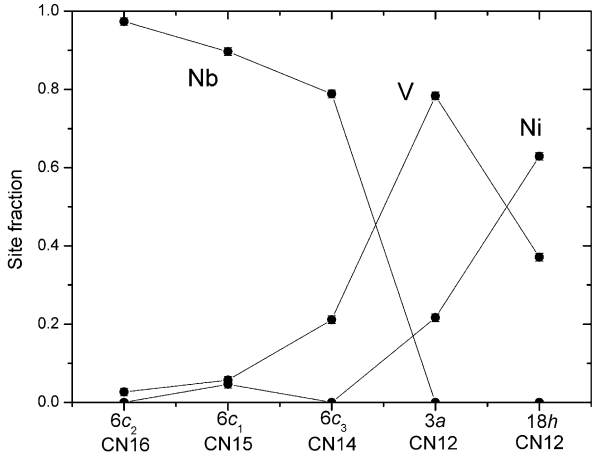


Fig. 4. Nb, V and Ni site fractions on the different sites obtained by joint refinement of neutron and X-ray powder diffraction data for the ternary compound $Nb_{42}Ni_{31}V_{27}$ (5).

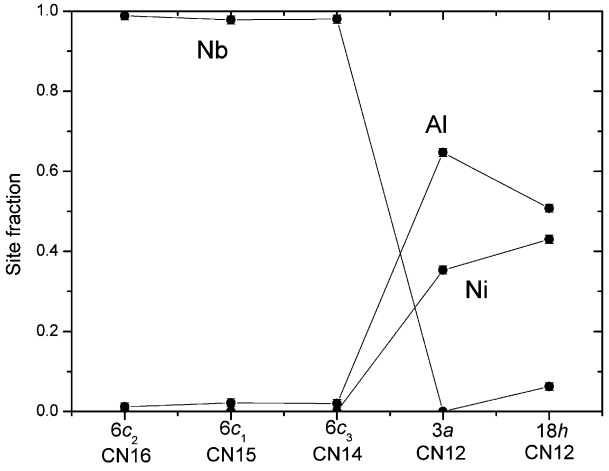


Fig. 5. Nb, Al and Ni site fractions on the different sites obtained by joint refinement of neutron and X-ray powder diffraction data for the ternary compound $Nb_{48}Ni_{23}Al_{29}$.

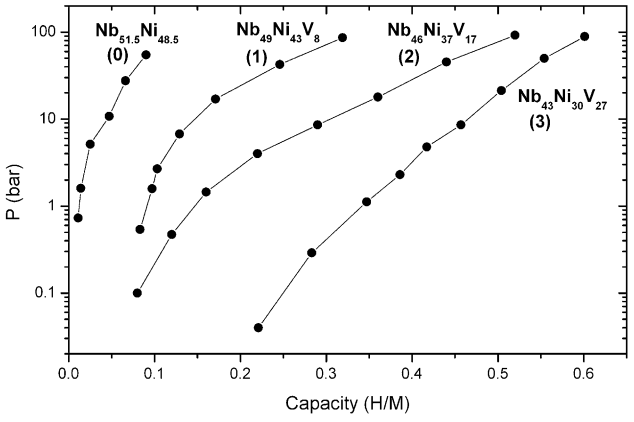


Fig. 6. Hydrogen absorption pressure–composition curves at 25 °C for the different $\mu$ phase samples in the Nb–Ni–V system. Data for the binary compound $Nb_{51.5}Ni_{48.5}$ [4] have been added for comparison.

Table 2
interstitial (all tetrahedral) sites in the $\mu$ phase structure. The coordination of the sites, position, and radius are reported. The two latter parameters have been calculated as the position and radius of the largest sphere in contact with the four coordination atoms in the structure of $Nb_{57}Ni_{43}D_{43.9}$ taking into account the lattice parameters and the composition weighted radius at the different metallic sites. The probability of finding $A_4$ ($A$ = Nb or V) in the coordination shell is calculated following the site distribution reported in Table 1

| Site | Coordination shell | | | | Wyckoff notation | Position | Radius (Å) | Probability for (Nb, V)$^4$ | | |
|---|---|---|---|---|---|---|---|---|---|---|
| | | | | | | | | $Nb_{57}Ni_{43}$ | $Nb_{42}Ni_{31}V_{27}$ | $Nb_{48}Ni_{23}Al_{29}$ |
| $D_1$ | 3*a* | 18*h* | 18*h* | 18*h* | 6*c* | 0, 0, $z = 0.940$ | $r = 0.27$ | 0 | 0.04 | 0 |
| $D_2$ | 6$c_1$ | 18*h* | 18*h* | 18*h* | 6*c* | 0, 0, $z = 0.232$ | $r = 0.36$ | 0 | 0.05 | 0 |
| $D_3$ | 6$c_1$ | 18*h* | 18*h* | 18*h* | 6*c* | 0, 0, $z = 0.899$ | $r = 0.36$ | 0 | 0.05 | 0 |
| $D_4$ | 6$c_2$ | 18*h* | 18*h* | 18*h* | 6*c* | 0, 0, $z = 0.281$ | $r = 0.35$ | 0 | 0.05 | 0 |
| $D_5$ | 6$c_1$ | 6$c_1$ | 6$c_3$ | 6$c_3$ | 18*g* | $x = 0.752$, 0, 1/2 | $r = 0.49$ | 0.74 | 0.88 | 0.92 |
| $D_6$ | 3*a* | 6$c_2$ | 18*h* | 18*h* | 18*h* | $x = 0.483$, $\bar{x}$, $z = 0.711$ | $r = 0.39$ | 0.01 | 0.11 | 0 |
| $D_7$ | 6$c_1$ | 6$c_3$ | 18*h* | 18*h* | 18*h* | $x = 0.459$, $\bar{x}$, $z = 0.780$ | $r = 0.40$ | 0.02 | 0.13 | 0 |
| $D_8$ | 6$c_1$ | 6$c_3$ | 18*h* | 18*h* | 18*h* | $x = 0.126$, $\bar{x}$, $z = 0.220$ | $r = 0.41$ | 0.02 | 0.13 | 0 |
| $D_9$ | 6$c_2$ | 6$c_2$ | 18*h* | 18*h* | 18*h* | $x = 0.138$, $\bar{x}$, $z = 0.294$ | $r = 0.44$ | 0.02 | 0.14 | 0 |
| $D_{10}$ | 6$c_2$ | 6$c_3$ | 18*h* | 18*h* | 18*h* | $x = 0.199$, $\bar{x}$, $z = 0.270$ | $r = 0.40$ | 0.02 | 0.14 | 0 |
| $D_{11}$ | 6$c_2$ | 6$c_3$ | 18*h* | 18*h* | 18*h* | $x = 0.533$, $\bar{x}$, $z = 0.730$ | $r = 0.40$ | 0.02 | 0.14 | 0 |
| $D_{12}$ | 3*a* | 6$c_2$ | 6$c_2$ | 18*h* | 36*i* | $x = 0.982$, $y = 0.301$, $z = 0.311$ | $r = 0.40$ | 0.09 | 0.29 | 0 |
| $D_{13}$ | 6$c_1$ | 6$c_1$ | 6$c_3$ | 18*h* | 36*i* | $x = 0.979$, $y = 0.313$, $z = 0.201$ | $r = 0.44$ | 0.11 | 0.34 | 0.06 |

Table 3
Crystal structure of the deuterides. Indicated are: the nominal composition (deuterium content measured by volumetry under the given pressure), lattice parameters, atomic positions for the metal atoms (occupancy parameters of the metal atoms are fixed to the values reported in Table 1), atomic positions ($^*$ not refined) and occupancy parameters for deuterium (in atom per site), displacement parameters, reliability factors and total refined deuterium content

| Nominal composition (at%) | $Nb_{57}Ni_{43}D_{44}$ (72.7 bar) | $Nb_{42}Ni_{31}V_{27}D_{64}$ (91.1 bar) | $Nb_{48}Ni_{23}Al_{29}D_{36}$ (95.8 bar) |
|---|---|---|---|
| Secondary phases | | | Nb(Al)$D_2$ (1 wt%) |
| $a$ (Å) ($\Delta a/a$) | 5.103(1) (+3.0%) | 5.136(1) (+3.9%) | 5.113(1) (+2.1%) |
| $c$ (Å) ($\Delta c/c$) | 27.649(3) (+2.5%) | 27.815(3) (+3.6%) | 27.926(3) (+2.5%) |
| $V$ (Å$^3$) ($\Delta V/V$) | 623.5(1) (+8.7%) | 635.3(1) (+11.9%) | 632.2(1) (+6.9%) |
| 3*a* | 0, 0, 0 | 0, 0, 0 | 0, 0, 0 |
| 6$c_1$ | 0, 0, $z = 0.1643(6)$ | 0, 0, $z = 0.1642(5)$ | 0, 0, $z = 0.1652(3)$ |
| 6$c_2$ | 0, 0, $z = 0.3500(6)$ | 0, 0, $z = 0.3514(5)$ | 0, 0,$z = 0.3513(3)$ |
| 6$c_3$ | 0, 0, $z = 0.4512(6)$ | 0, 0, $z = 0.4510(6)$ | 0, 0, $z = 0.4514(3)$ |
| 18*h* | , $\bar{x}$, $z = 2544(2)$ | $x = 0.8315(15)$, $\bar{x}$, $z = 0.2555(3)$ | $x = 0.8325(13)$, $\bar{x}$, $z = 0.2581(3)$ |
| $D_4$ (6*c*) | | 0, 0, $z = 0.281^*$ | |
| | | D 0.4(1) | |
| $D_5$ (18*g*) | $x = 0.730(6)$, 0, 1/2 | $x = 0.725(9)$, 0, 1/2 | $x = 0.727(3)$, 0, 1/2 |
| | D 4.6(2) | D 3.4(1) | D 7.0(1) |
| $D_6$ (18*h*) | | $x = 0.483^*$, $\bar{x}$, $z = 0.711^*$ | $x = 0.483^*$, $\bar{x}$, $z = 0.711^*$ |
| | | D 0.4(1) | D 0.7(1) |
| $D_7$ (18*h*) | $x = 0.459^*$, $\bar{x}$, $0.780^*$ | $x = 0.459^*$, $\bar{x}$, $z = 0.780^*$ | |
| | D 0.6(2) | D 0.6(2) | |
| $D_8$ (18*h*) | | $x = 0.126^*$, $\bar{x}$, $z = 0.220^*$‘D 0.6(2) | |
| $D_9$ (18*h*) | | | $x = 0.138^*$ $\bar{x}$, $z = 0.294^*$ |
| | | | D 0.3(1) |
| $D_{10}$ (18*h*) | | $x = 0.199^*$, $\bar{x}$, $z = 0.270^*$ | $x = 0.199^*$, $\bar{x}$, $z = 0.270^*$ |
| | | D 1.2(1) | D 0.6(1) |
| $D_{11}$ (18*h*) | $x = 0.533^*$, $\bar{x}$, $0.730^*$ | $x = 0.533^*$, $\bar{x}$, $z = 0.730^*$ | $x = 0.533^*$, $\bar{x}$, $z = 0.730^*$ |
| | D 0.5(2) | D 1.7(2) | D 0.3(1) |
| $D_{12}$ (36*i*) | $x = 0.990(9)$, $y = 0.291(11)$, $z = 0.303(2)$ | $x = 0.978(5)$, $y = 0.284(6)$, $z = 0.312(1)$ | $x = 0.982^*$, $y = 0.301^*$, $z = 0.312(3)$ |
| | D 5.6(3) | D 9.2 (2) | D 1.6(1) |
| $D_{13}$ (36*i*) | $x = 0.979^*$, $y = 0.313^*$, $z = 0.199(3)$ | $x = 0.974(6)$, $y = 0.297(5)$, $z = 0.201(1)$ | $x = 0.979^*$,$y = 0.313^*$,$z = 0.205(2)$ |
| | D 3.8(3) | D 9.2(2) | D 2.5(1) |
| $B_{3a,\ 18h}$ | 2.19(3) | 1.17(3) | 0.98(3) |
| $B_{6c1,\ 6c2,\ 6c3}$ | 2.63(5) | 0.81(3) | 0.61(2) |
| $B_D$ | 2.22(23) | 2.59(12) | 1.33(11) |
| $\chi^2$ | 4.9 | 4.2 | 5.6 |
| $R_{Bragg}$ (%) | 11.6 | 7.5 | 7.4 |
| Total D refined (D/cell)/(D/M) | 15.1(12)/0.39(3) | 26.2(15)/0.67(4) | 13.1(8)/0.34(2) |

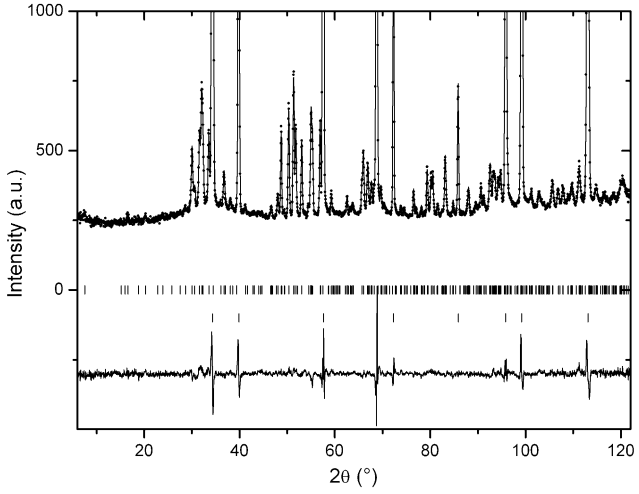


Fig. 7. Rietveld refinement of $Nb_{42}Ni_{31}V_{27}D_{64}$ under 91.1 bar. The observed pattern (dots), the calculated curve (line), the difference curve (line below) and the reflection positions (vertical bars) are plotted. The second phase corresponds to the austenitic stainless-steel container.

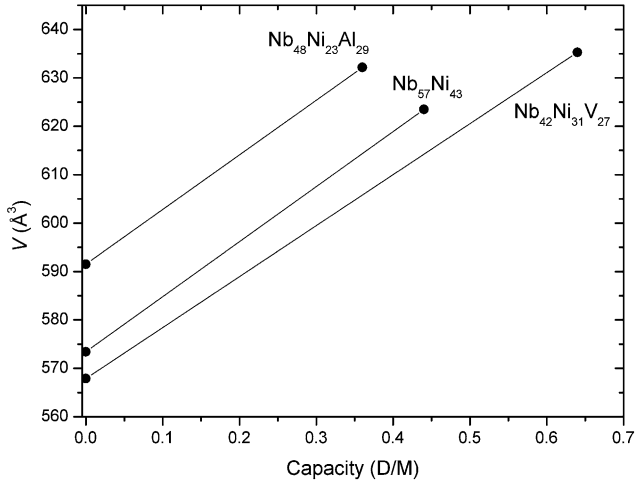


Fig. 8. Cell volume as a function of the nominal deuterium content for the three studied compounds. The error bars are smaller than the dot size.

deduce from the slopes the average atomic volume for deuterium in the $\mu$ phase structure. This volume of 2.8 $Å^3$/atom is in close agreement with the volume observed in other metal hydrides [9].

## 4. Discussion

The phase diagram data from the present work on the Nb–Ni–V system generally corroborate the findings of Eremenko et al. [7] but give a more accurate picture in the region of the $\mu$ phase domain. The sample $Nb_{41}Ni_{26}V_{33}$ (4) stands in the tie-triangle with $\mu$, C14 and bcc, but close to the $\mu$-C14 tie-line. This result allows to define more accurately the equilibrium compositions of the three phases, particularly those of $\mu$ and C14 which can be found in Table 1. On the other hand, the comparison of the results between the two samples $Nb_{43}Ni_{30}V_{27}$ and $Nb_{42}Ni_{31}V_{27}$ in equilibrium with bcc and C14, respectively allows to draw a more narrow extension of the $\mu$ homogeneity range than previously reported.

The cell volume of the $\mu$ phase plotted as a function of the V composition (Fig. 2) follows a regular increase, in agreement with the fact that the compositions studied follow a straight line in the ternary composition diagram. This behavior has for most probable explanation a linear dependence of the cell volume as a function of both Ni and V compositions. One may note that the extent of the lattice parameter variation along the ternary domain is rather weak as compared with the variation observed in the Nb–Ni binary system [2] (see Fig. 2). The increase of the cell volume induced by V substitution (with atomic radius $R = 1.34$ Å) to Ni ($R = 1.24$ Å) is compensated in some way by the decrease in the Nb ($R = 1.46$ Å) content imposed by the shape of the $\mu$ phase homogeneity domain.

A thorough investigation of the order in binary $\mu$ phases (in Nb–Ni [2], Mo–Co, Ta-Ni and Mn–Si [3] systems) was previously conducted. The main results can be briefly summarized. The $\mu$ phase, like many Frank–Kasper phases (e.g. $A15$ and $\sigma$ phases) is formed in transition metal $A$–$B$ systems where $A$ is an early transition metal, crystallizing in the bcc structure and $B$ a late transition metal, smaller in size, crystallizing in the fcc structure. The $A$ atom has a strong preference for the sites with high coordination number (CN), i.e. $6c_1$ (CN 15), $6c_2$ (CN 16) and $6c_3$ (CN 14), while the $B$ atom prefers the sites with low coordination $3a$ (CN 12) and $18h$ (CN 12). The $\mu$ phase exists at compositions ranging from 39 to 59 at% $A$ (if one excludes the peculiar case of $\mu$ Mn–Si). The non-stoichiometry is accommodated by substitutional disorder. Site $6c_3$ is never found to be fully occupied by $A$ and is complemented by $B$ whatever the composition. For compositions rich in $A$, $A$ atoms replace $B$ atoms on the two sites with coordination 12, but unequally and with a strong preference for site $3a$.

One of the aims of this work was to study the ordering behavior in ternary compounds. This was actually made for two ternary substitutions by Al and V. The plot in Fig. 3 allows to follow the Nb occupancy when V progressively enters the lattice. The results are incomplete since the distribution of V and Ni could not be obtained. However, it helps to understand how the sites are gradually left by Nb. Nb atoms in sites $3a$ and $18h$ are progressively replaced leaving an almost fully ordered Nb distribution at the composition $Nb_{46}Ni_{37}V_{17}$ (2). Indeed, for this composition, Nb fully occupies the three sites of high coordination and is absent from the two sites of low coordination. For lower Nb content, it can clearly be seen that site $6c_3$ with CN

14 begins to be depleted in Nb atoms. A more complete view is obtained for $Nb_{42}Ni_{31}V_{27}$ (5) since, for this sample, the distribution of the three atoms has been obtained by a joint refinement of X-ray and neutron powder diffraction data. The corresponding site fractions have been plotted for the different sites in Fig. 4. The obtained results follow the rule stating that larger atoms prefer the sites with the highest coordination. It is remarkable that the rule is followed not only for Nb, but also for V which has an intermediate radius between Nb and Ni. As already noted in the case of the binary Nb–Ni compounds [2], the two sites 3*a* and 18*h*, both with CN 12, follow different behavior, site 3*a* having stronger tendency to accommodate larger atoms. This may be related to differences in distances to nearest neighbors [2] or to electronic properties [10].

The same kind of data has been obtained for a ternary compound with Al ($Nb_{48}Ni_{23}Al_{29}$). Though the same trends are observed, the following differences may be noted. The Nb content being larger, Nb fully occupies site $6c_3$. The distribution of Al and Ni on the two sites with CN 12 is more homogeneous than in the case of V. A brief comment may be made on the character of each atom. The shape of the ternary field in the Nb–Ni–Al system [11], the fact that Al acts as a *B* element in, e.g. *A*15 and $\sigma$ Nb–Al and the fcc crystal structure of this element allow to classify Al as a *B* element. One may note also that Si, another *p* element is a *B* element in $\mu$ Mn–Si [3]. The ordering scheme found in the ternary compound with nearly similar distribution of Al and Ni is in favor of this classification which relies more on the electronic than on the geometric point of view (Al has an atomic radius ($R = 1.43$ Å) closer to Nb ($R = 1.46$ Å) than to Ni ($R = 1.24$ Å)). The case is more complex for V. On the one hand V is an *A* atom from the electronic point of view (it lies in the same column as Nb, it crystallizes in the bcc structure and it has a tendency to act as an *A* element in, e.g. *A*15 and $\sigma$ V–Ni). But, on the other hand, the shape of the $\mu$ phase ternary field in the Nb–Ni–V system, the absence of any binary $\mu$ phase with V and the rather small radius compared to that of Nb indicate that it may act as a *B* element. A confirmation is given by the present results on the distribution of this atom which is found to be close to that of Al, i.e. strongly different from the one of Nb.

The pressure–composition hydrogen absorption curves for the compounds in the Nb–Ni–V system do not evidence any pressure plateau which would indicate a phase transition to a distinct hydride phase. On the contrary, in the pressure range investigated, a solid solution behavior is observed. One may note the remarkable increase of the hydrogen storage capacity with V substitution. For the compound $Nb_{43}Ni_{30}V_{27}$ (3), the hydrogen uptake is even larger than for the Nb richest $\mu$ phase previously reported ($Nb_{56.9}Ni_{43.1}H_{52}$ [5]). To elucidate the reasons for this increase, neutron diffraction experiments were undertaken.

Whatever the sample, it is found that the most occupied sites are $D_5$, $D_{12}$, and $D_{13}$. One may note that the radius of those three sites is above the 0.4 Å limit, a necessary condition for being occupied [12]. However, not all the sites with a radius larger than 0.4 Å are occupied. Site $D_{13}$ with the same size as $D_9$, and $D_{12}$ with a size similar to sites $D_6$ and $D_{11}$ are much more occupied, showing that the size criterion is not predominant. $D_5$, $D_{12}$, and $D_{13}$ are the three sites coordinated by only one or no metal atom in the 18*h* position. This latter site is less prone to accept Nb which has the highest affinity for hydrogen. We have therefore concluded that the chemical affinity of the insertion sites should therefore be investigated. This can be easily done after obtaining the metal atom occupancy parameters for the metallic compounds. Nb and V (hereafter called *A* elements) are contrary to Al and Ni the two atoms having a strong affinity for hydrogen. This can be inferred from the enthalpy of formation of $MH_{0.5}$ which is −38, −42, −3 and −7 kJ/mol H for $M =$ Nb, V, Ni and Al, respectively [13]. The probability reported in Table 2 of finding an $A_4$ tetrahedron in the coordination shell of each deuterium site has been calculated following:

$$(p^{i}_{Nb} + p^{i}_{V})(p^{ii}_{Nb} + p^{ii}_{V})(p^{iii}_{Nb} + p^{iii}_{V})(p^{iv}_{Nb} + p^{iv}_{V}) \quad (1)$$

where *i*, *ii*, *iii*, and *iv* represent the four metal sites in the coordination shell $p^{i}_{A}$ represents the probability of finding the atom *A* on site *i*, i.e. the site fraction.

In the case of $Nb_{57}Ni_{43}$, the largest probability of finding $Nb_4$ tetrahedron is for site $D_5$ which is actually found to be the most occupied. Non-negligible probability occurs also on sites $D_{12}$ (9%) and $D_{13}$ (11%) which are also found to be significantly occupied with a similar order of magnitude (16% and 11%).

Vanadium is, like niobium, an element having a strong affinity for hydrogen. In the ternary compound, it replaces a significant quantity of nickel on site18*h*. This has for consequence a much stronger probability of finding $A_4$ coordination around the deuterium sites coordinated by a metal atom in 18*h*. This is particularly the case for sites $D_{12}$ and $D_{13}$ which have a large probability of being of the $A_4$ type (29% and 34%) in $Nb_{42}Ni_{31}V_{27}$. This explains the spectacular increase of the occupancy of these sites which are found to follow even quantitatively this trend (occupancy of 26%). Following the so-called Switendick criterion [12,14] the presence of a deuterium atom inhibits the occupancy of other sites at a distance less than 2.1 Å. In this frame, the decrease of the occupancy of site $D_5$ may be understood if one considers the blocking effect that could be imposed on this latter site by strong deuterium occupancy of site $D_{13}$ since it possesses three sites $D_5$ at a distance inferior to 2.1 Å. One may also note partial

occupancies in sites $D_6$–$D_{11}$ well accounted for by the non-negligible probability of finding $A_4$ in the coordination shell.

Concerning the aluminum compound, one may observe that the occupancy on site $D_5$ increases notably. This has to be related with the pronounced order of Nb atoms on sites $6c_1$ and $6c_3$ which coordinate this deuterium insertion site. Indeed, more niobium atoms occupy $6c_3$ than in the binary $Nb_{57}Ni_{43}$ in spite of much lower Nb concentration. This has for a result that $D_5$ in this compound has the highest probability to be coordinated by four Nb atoms among all the compounds studied. However, no more than half of the $D_5$ sites may be occupied simultaneously if the 2.1 Å rule is followed. Aluminum, contrarily to vanadium, is known to have, like other *p* elements, a strong repulsive effect on hydrogen see e.g. in $LaNi_5$ substituted compounds [15], in Laves phases [16], and other compounds [17,18]. A large occupancy of this atom on site 18*h* has for a consequence a large diminution of the deuterium occupancy parameters on the deuterium sites coordinated by this metal site. Only $D_{13}$ remains with a significant probability of finding $Nb_4$ as a coordination shell, once again in agreement with the observed occupancy (7%).

The $\mu$ phase hydrogenation capacities measured in the systems Nb–Ni, Nb–Ni–Al and Nb–Ni–V as a function of composition may now be rationalized. The significant increase of the storage capacity in Nb–Ni system as a function of Nb content (from 0.10 H/M for $Nb_{51.5}Ni_{48.5}$ to 0.52 H/M for $Nb_{56.9}Ni_{43.1}$ [5]) may be attributed to the progressive replacement of Ni by Nb on site 18*h* (from 1.2 to 2.9 atom/site) and by the related probability increase of finding $Nb_4$ coordination shell around $D_{12}$ and $D_{13}$. The relatively constant capacity when Al is substituted (0.52 H/M for $Nb_{55}Ni_{35}Al_{10}$, 0.45 for $Nb_{50}Ni_{30}Al_{20}$ and 0.41 H/M for $Nb_{46.6}Ni_{22.1}Al_{31.3}$ [5]) is explained by the fact that Al does not occupy sites $6c_1$ and $6c_3$ leaving site $D_5$ available for deuterium insertion in spite of the strong repulsive effect of Al. The remarkable increase of hydrogen capacity between $Nb_{51.5}Ni_{48.5}$ and $Nb_{43}Ni_{30}V_{27}$ on the pressure–composition curves studied in this work should be understood by the progressive filling of the 18*h* sites by V and the creation of $A_4$ environment for the positions $D_{12}$ and $D_{13}$ in an even more pronounced manner than in the Nb–Ni binary system. For this reason, the largest capacity is obtained for this system. Finally, one should observe that the changes of occupancy cannot be accounted for by the variations of the site radius induced by substitution. If larger sites in the case of $Nb_{42}Ni_{31}V_{27}D_{64}$ as compared to $Nb_{57}Ni_{43}D_{44}$ ($r(D_5) = 0.51$ Å, $r(D_{12}) = 0.42$ Å, $r(D_{13}) = 0.46$ Å) could account for larger occupancies on sites $D_{12}$ and $D_{13}$, it does not explain the smaller occupancy on site $D_5$. Similarly, if smaller sites in the case of $Nb_{48}Ni_{23}Al_{29}D_{36}$ ($r(D_5) = 0.48$ Å, $r(D_{12}) = 0.39$ Å, $r(D_{13}) = 0.43$ Å) could account for lower occupancy on sites $D_{12}$ and $D_{13}$, it does not explain the larger occupancy on site $D_5$. Again, the size criterion describes worse the deuterium occupancies than the chemical affinity of the insertion sites.

## 5. Conclusion

Though not presenting very interesting capacities for applications (the highest capacity obtained is 0.9 wt%), the $\mu$ phase hydrides are very interesting to understand the intimate behavior of metal hydrides. They can be considered as model systems because they belong to Frank–Kasper phases and, thus, present only tetrahedral interstices, they are partly disordered phases in binary systems and, finally, because the ternary substitution is not found to be a replacement of only one atom in the studied ternary systems. It has been found to be extremely useful to study the distribution of the metallic atoms in the case of ternary substitutions. This is a difficult task since one must use joint refinement of diffraction data obtained by different methods (e.g. X-ray and neutron or X-ray at various wavelengths including near edge measurement). But, this may explain the behavior in the deuterides even, or perhaps even more, in the case of a complex crystal structure. Capacities, deuterium locations and occupancies can be fairly well rationalized considering only two criteria: the location of deuterium in sites coordinated by $A_4$ and the so-called Switendick criterion of a minimum distance between deuterium atoms. They can be explained by the crystal atomic distribution and not by the only chemistry since one would have expected a priori a much more pronounced diminution of the capacity after aluminum substitution and a stronger increase after vanadium substitution. The size criterion for the deuterium insertion sites has been shown to be a necessary but not sufficient condition for a site to be occupied. Moreover, increase of the site radius by substitution does not result necessarily in an increase of the occupancy. The criterion of chemical affinity explains better the observed behavior.

## Acknowledgments

The author wishes to acknowledge N. Ulusoy for help with the synthesis of some samples, F. Briaucourt for technical assistance, E. Leroy for the EPMA measurements and F. Bourée-Vigneron from the Laboratoire Léon Brillouin for the neutron diffraction measurements.

## References


[1] H. Arnfelt, A. Westgren, Jernkontorets Ann. 119 (1935) 185–196.
[2] J.-M. Joubert, Y. Feutelais, Calphad 26 (3) (2002) 427–438.
[3] J.-M. Joubert, N. Dupin, Intermetallics 12 (2004) 1373–1380.
[4] J.-M. Joubert, A. Percheron-Guégan, J. Alloys Compd. 317–318 (2001) 71–76.
[5] J.-M. Joubert, C. Pommier, E. Leroy, A. Percheron-Guégan, J. Alloys Compd. 356–357 (2003) 442–446.
[6] J. Rodríguez-Carvajal, Proceedings of the XV Congress of International Union of Crystallography, Satellite Meeting on Powder Diffraction, Toulouse, France, 1990, p. 127.
[7] V.N. Eremenko, S.B. Prima, L.A. Tret'yachanko, P.A. Verkhovodov, Sov. Powder Metall. Met. Ceram. 25 (12) (1986) 977–981.
[8] H. Müller, K. Weymann, J. Less-Common Met. 119 (1986) 115–126.
[9] Y. Fukai, The metal–hydrogen system, in: U. Gonser (Ed.), Springer Series in Materials Science, vol. 21, Springer, Berlin, 1992.
[10] M. Sluiter, A. Pasturel, Y. Kawazoe, Phys. Rev. B 67 (2003) 174203.
[11] N. Saunders, Aluminium–niobium–nickel, in: G. Petzow, G. Effenberg (Eds.), Ternary Alloys, MSI, VCH, 1993, pp. 348–357.
[12] D.G. Westlake, J. Less-Common Met. 90 (1983) 251–273.
[13] R. Griessen, T. Riesterer, Hydrogen in intermetallic compounds I, in: L. Shlapbach (Ed.), Topics in Applied Physics, vol. 63, Springer, Berlin, 1988.
[14] A.C. Switendick, Z. Phys. Chem. Neue Folge 117 (1979) 89–112.
[15] H. Diaz, A. Percheron-Guégan, J.-C. Achard, C. Chatillon, J.-C. Mathieu, Int. J. Hydrogen Energy 4 (5) (1979) 445–454.
[16] M. Bereznitsky, I. Jacob, J. Bloch, M.H. Mintz, J. Alloys Compd. 346 (2002) 217–221.
[17] S. Rundqvist, R. Tellgren, Y. Andersson, J. Less-Common Met. 101 (1984) 145–168.
[18] N.J. Clark, E. Wu, J. Less-Common Met. 163 (1990) 227–243.